4 November 1983, Volume 222, Number 4623 SCIENCE

Three Mars Years: Viking Lander 1 Imaging Observations

Raymond E. Arvidson, Edward A. Guinness
Henry J. Moore, James Tillman, Stephen D. Wall

The Mutch Memorial Station (Viking Lander 1) touched down on Mars on 20 July 1976 and successfully completed 2245 Mars sols or 3.3 years of operation before contact was lost on 13 November 1982 (*1, 2*). In this article we discuss the imaging and meteorological observations (*3, 4*) that are pertinent to understanding the relation between weather systems and the manner in which surface materials are redistributed. We begin with a summary of the strategy used in monitoring the martian environment from the Mutch Memorial Station. We then examine changes in surface contrast induced by aeolian phenomena, describe evidence for stripping of centimeters of disturbed soil in selected regions, and discuss the probable weather systems that caused the changes. We end with a section on implications for the evolution of the martian surface.

Summary. The Mutch Memorial Station (Viking Lander 1) on Mars acquired imaging and meteorological data over a period of 2245 martian days (3.3 martian years). This article discusses the deposition and erosion of thin deposits (ten to hundreds of micrometers) of bright red dust associated with global dust storms, and the removal of centimeter amounts of material in selected areas during a dust storm late in the third winter. Atmospheric pressure data acquired during the period of intense erosion imply that baroclinic disturbances and strong diurnal solar tidal heating combined to produce strong winds. Erosion occurred principally in areas where soil cohesion was reduced by earlier surface sampler activities. Except for redistribution of thin layers of materials, the surface appears to be remarkably stable, perhaps because of cohesion of the undisturbed surface material.

Monitoring Strategy

Acquisition of imaging data for the first 43 sols was directed toward covering the scene in color and high-resolution modes (*5*). A considerable amount of meteorological data were also collected (*4*). In addition, images were obtained in support of acquisitions of soil samples for the biology, molecular analysis, and inorganic chemical analysis experiments (*6*). Samples were collected with a surface sampler capable of reaching 3.7 m from the lander and covering 160° in azimuth (Fig. 1). Before being stowed on Sol 639, the surface sampler was also used to expose materials beneath rocks, to investigate physical and magnetic properties, and to construct five piles of surface materials in order to monitor wind erosion (*3*).

On Sol 921 the lander was programmed to an automated state in which an image of the surface and sky, together with meteorological data and engineering information, were recorded on a tape recorder and transmitted directly back to Earth roughly once a week. Five images covering selected parts of the scene were acquired during each 37-sol period. Two of the images were acquired in color and repeated every 37 sols. Acquisition of the other three images was designed so that 54 separate frames were acquired over one martian year, with a repeat period of 1 year. Thus the imaging sequence was designed to monitor both short-term (tens of sols) and yearly changes. An important aspect of the images that repeated on a yearly cycle was that they were acquired at nearly the same solar incidence, emission, and phase angles, thereby minimizing photometric effects that complicate the search for changes in surface brightness and color.

Meteorological data returned during the automatic mission included atmospheric pressures and temperatures sampled approximately once an hour, an hourly temperature reading from a sensor located on one of the footpads, and wind velocities sampled approximately once every few hundred seconds.

Contrast Changes in Surface Materials

The major meteorological events of the first year of observations were two global dust storms, one beginning in the northern fall and one in the northern winter. Each storm lasted about 100 sols (*3*). Atmospheric optical depths were measured by cameras before, during, and after the storms by directly imaging the sun. The maximum optical depths exceeded values of 5 to 8, as compared to 0.5 before and after the storms (*3*). In addition to the global storms, a local storm passed over the site on Sol 423 (*7*), but without significantly altering the surface. Images acquired at similar lighting conditions before and after the two global storms show that the surface was discernibly brighter and redder after the storms had cleared, probably because of the deposition of a dust layer, tens to hundreds of micrometers thick (*3*).

The time line for images acquired with similar lighting conditions can now be extended over three martian years (*8*).

R. A. Arvidson is an associate professor and E. A. Guinness is a senior research associate in the Department of Earth and Planetary Sciences, Washington University, St. Louis, Missouri 63130. H. J. Moore is a geologist with the U.S. Geological Survey, Menlo Park, California 94025. J. Tillman is a meteorologist in the Department of Atmospheric Sciences, University of Washington, Seattle 98195. S. D. Wall is a research engineer at the Jet Propulsion Laboratory, Pasadena, California 91109.

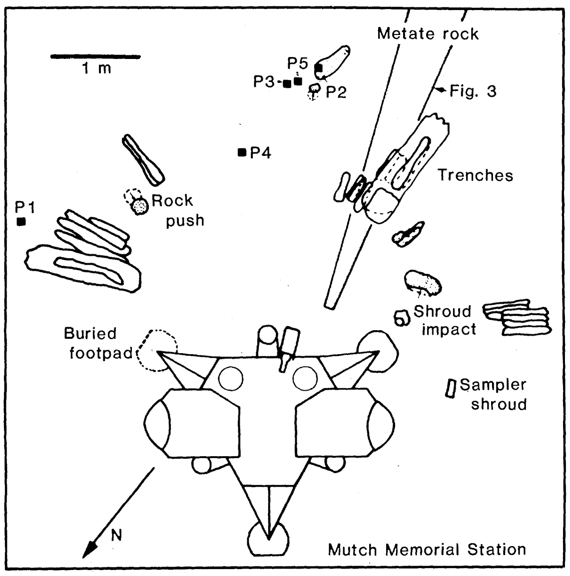

Fig. 1. Overhead view of Lander 1 and immediate surroundings. Location of trenches, places where rocks were pushed, and piles (*P1*, *P2*, and so on) constructed by the surface sampler are shown. The sampler was turned off on Sol 639 and the features produced during the various experiments were monitored until Sol 2245 to evaluate aeolian processes on Mars.

The location of one such image set is shown in a panoramic view of the landing site in Fig. 2 and as side-by-side comparisons of the 3 years of data in Fig. 3. The minimum brightness values for each frame in Fig. 3 occur in shadows cast by rocks, that is, areas illuminated only by skylight. The minima are statistically indistinguishable for the four frames (*9*). The similarity in minimum brightness values indicates that the extent of atmospheric attenuation and scattering of sunlight by aerosols were similar. Thus, variations in brightness and contrast among the images must be due to differences in the reflectance of surface materials.

The images in Fig. 3 show a surface that was initially dark, with a moderate amount of contrast. The surface then became brighter and contrast was reduced after the first winter and the two global storms. A number of regions were then disturbed by surface sampling activities. These disturbed areas are evident as darker regions in the frame acquired at the end of the first year. By the end of the second year these disturbed regions had lost most of their contrast relative to surrounding regions, suggesting the addition of a second thin layer of bright dust by deposition from a dust storm or storms during the second year. Such an inference is supported by the presence of strong diurnal and semidiurnal pressure oscillations during part of the second winter, oscillations that imply a global dust storm but one of lower intensity than those of the first year (*10*). The visual impression gained by comparing images acquired at the end of the second as opposed to the third year is that the scene became darker and the contrast increased sometime between the second and third years. This impression is corroborated by quantitative examination of the distribution of brightness values for the four frames, which show a 30 percent decrease in brightness and a 50 percent increase in contrast between the second and third years. If the observations over the 3 years are interpreted in terms of deposition and removal of thin layers of dust, then erosion of the bright dust layers dominated the third year.

Changes in Surface Morphology

Approximately 2½ martian years after landing, the station witnessed significant changes in surface morphology that can be attributed to high winds. The changes in scene contrast and brightness discussed in the previous section were caused by the redistribution of dust layers perhaps tens to hundreds of micrometers in thickness. On the other hand, changes in morphology would indicate a greater extent of redistribution, since such changes must be at least several millimeters in dimension to be discerned by the cameras. Five conical piles of soil (*11*) were constructed by the surface sampler during the first year. These piles were imaged during the remainder of the mission to detect morphological changes and thus to calibrate the rate of soil erosion by winds. During construction, fines dropped from the surface sampler formed dark-appearing deposits on the downwind side of the piles, but the bulk of the materials formed cones 3 to 5 cm tall and 5 to 10 cm wide.

The first conical pile was constructed with fine-grained material during the dust storms of the first year. The site was chosen to be out of the turbulent wake of the lander, under the assumption that the highest wind velocities correspond to the direction inferred from wind tails seen extending from many rocks. The darkened surface around the pile disappeared within a few hundred sols, probably because of deposition associated with fallout from the global dust storms. The last high-resolution picture of pile 1 was taken on Sol 921, and no changes in morphology were discernible. Thus, pile 1 survived both the global and the local storms of the first year.

Conical pile 4 was constructed next to a rock, partly covering it with soil material (Fig. 4). The initially darkened surface disappeared within 100 sols. The relief and form of the pile appeared unchanged in pictures taken just before the second winter (Sol 921). The next picture of the pile, taken during the third winter (Sol 1765), shows that its relief had been reduced and its form altered during the third winter. Changes in the pile indicate that eroding winds came from an easterly direction. In addition, a number of soil clods 4 to 5 mm in diameter that were deposited on the surface as a result of sampler activities were also removed.

Conical piles 2 and 3 were constructed on a rock and among rocks and pile 5 was constructed nearby with relatively blocky material (Fig. 5). Pile 2, which was perched precariously on the edge of an 18-cm-high rock, did not have a darkened surface but rather fines were draped over the left side and on top of the rock. The darkened surfaces associated with piles 3 and 5 disappeared within a few hundred sols. The shape and form of these three piles and surrounding fine-grained deposits appeared to be unchanged on Sol 921 as well as on Sols 1543 and 1601. However, the deposits were almost entirely removed sometime between Sol 1601 and the next time the area was imaged, on Sol 2068. For pile 3, only a residue composed of a few clods was left, while a small mound of fragments was left at the site of pile 5. Pile 2 material was completely removed.

If it is assumed that piles 2, 3, 4, and 5 were altered as a result of the same wind event, then the change must have occurred between Sols 1601 (piles 2, 3, and 5 unchanged) and 1765 (pile 4 changed). Significant wind erosion during the third year is also demonstrated by the changes in brightness and contrast, which show that the bright dust layers from dust storms were largely removed during the third winter (Fig. 3).

Significant changes occurred elsewhere on the surface during the third winter. Fragile soil clods and platy fragments were destroyed or removed near one of the footpads. Ripple-like bed forms with a wavelength of several centimeters appeared in several places. Near pile 2, a fragment several centimeters wide and perched atop a larger one was rotated; nearby soil clods were reduced and partly removed, and the local surface was lowered. Rims of two small trenches were extensively eroded, and the shape of a small impact crater was altered. Importantly, a small (about 3-cm-wide) rock or clod was moved some-

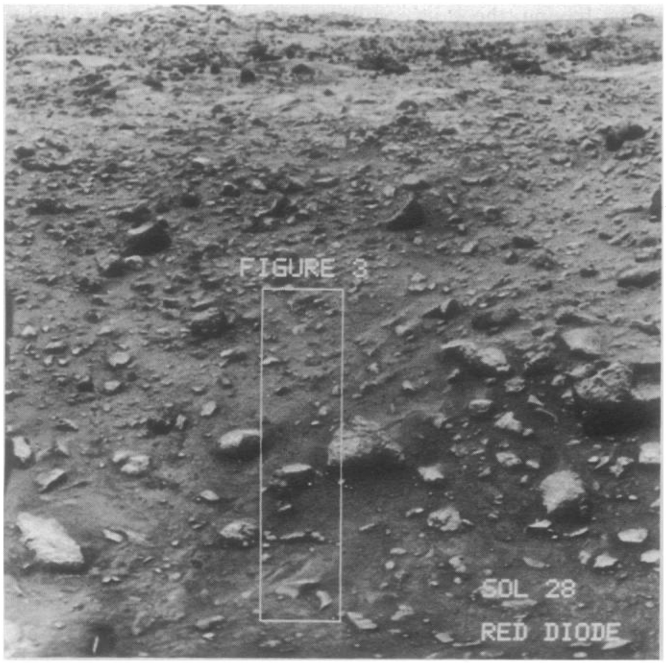

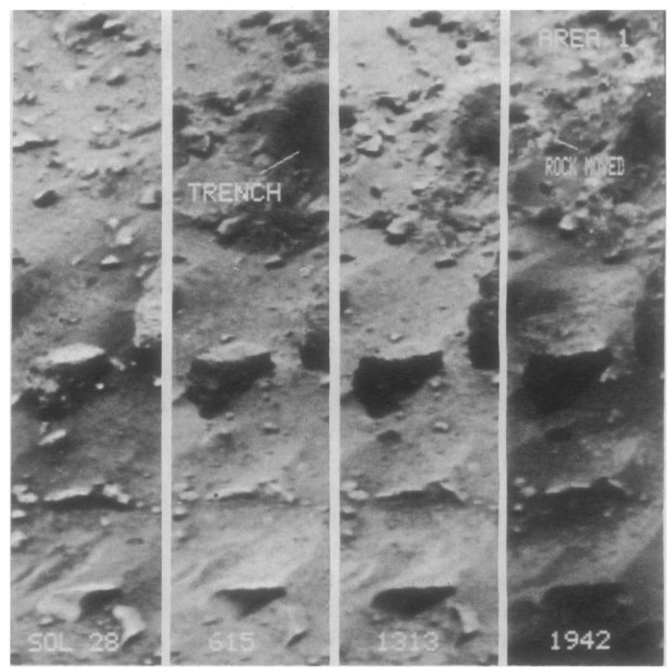

Fig. 2 (left). Panoramic view by camera 2, showing the location of one of the regions that have been monitored repeatedly during the mission. The 3 years of data for this region are shown in Fig. 3. (Frame A168, acquired on Sol 28.) Fig. 3 (right). Lander 1 frames acquired with the red diode on Sols 28, 615, 1313, and 1942, with nearly identical lighting conditions. Trenching and other activities occurred after the two global dust storms of the first year. Note the small rock or clod, about 3 cm across, that was moved between Sols 1313 and 1942. (Frames A168, H196, J063, and J153.)

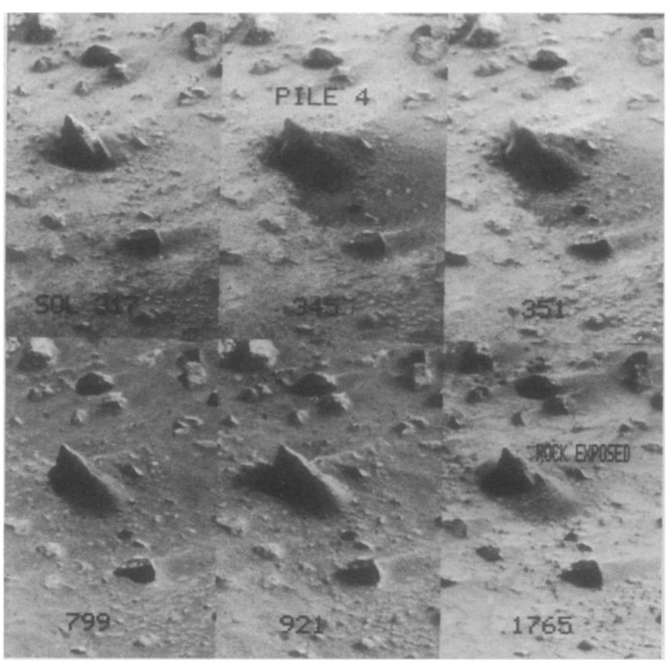

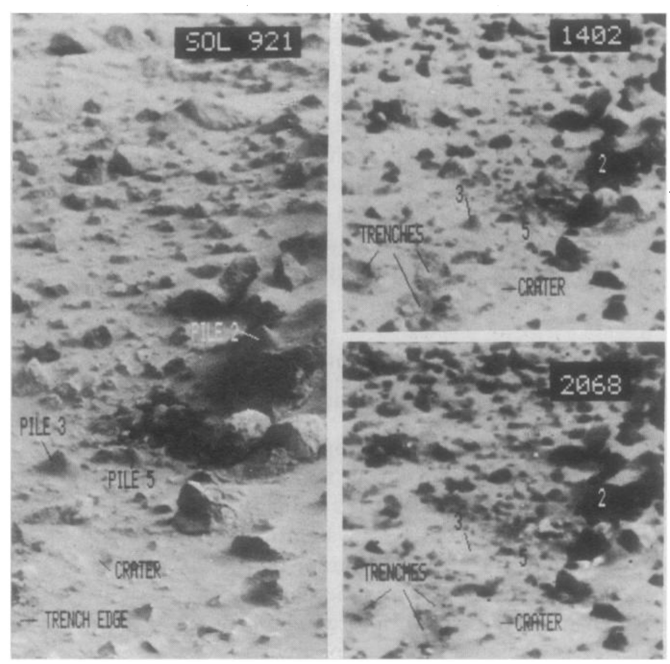

Fig. 4 (left). Sequence of six images covering pile 4 before and after time of construction. Note the contrast reduction from Sols 351 to 799. Between Sols 921 and 1765 the contrast increased and the pile shape changed. (Frames D183/317, E054/356, E082/351, I159/799, J007/921, and J130/1765, where the numerator is the frame number and the denominator is the Sol of acquisition.) Fig. 5 (right). Sequence of images showing the removal of piles 2, 3, and 5 between Sols 1402 and 2068. The left-hand image was acquired in the high-resolution mode (0.04°), while the right-hand images were acquired in the low-resolution mode (0.12°). These data, together with a high-resolution image acquired on Sol 2209, document the removal of the piles, alteration of trenches, and extensive wind erosion of that part of the surface modified by surface sampler activities. (Images J013, J081, and J171.)

time between Sols 1720 and 1757 (Fig. 3). The movement of the rock, the alterations of the conical piles, clods, trenches, and other features, and the increase in scene contrast demonstrate that an erosion event or events of substantial magnitude occurred during the third winter season, probably between Sols 1720 and 1757.

Short-Term Changes in Scene Radiance

There are no direct measurements of atmospheric opacity beyond Sol 921, when the last image of the sun was acquired. There are, however, a number of images of the sky and surface that were acquired with similar solar incidence, emission, and phase angles that can be used to monitor changes in overall scene radiance caused by changes in atmospheric opacity. For instance, Fig. 6 shows a sequence of three frames acquired during the third winter on Sols 1705, 1742, and 1853. Radiance is roughly two times lower for the middle frame than for the other two. In addition, the relative brightness of the sky increases upward in the middle frame, whereas it decreases upward in the other two frames, suggesting a change in the abundance and vertical distribution of atmospheric dust. The decrease in radiance corresponds in time to the approximate range of sols when the contrast of the scene increased, the piles were eroded, the rocks moved, and a ripple morphology appeared.

Similarly, images acquired on Sols 2209 and 2230 show a decrease in radiance as compared to a frame acquired on Sol 2201. The last data from the lander were received on Sol 2245, and insufficient image data were collected to document surface changes that may have occurred near the end of the mission.

Imaging Results and Temperature, Pressure, and Wind Velocity Data

Meteorological data corroborate that the late winter season during the third year was unusual. The period roughly between Sols 1720 and 1760 was a time of low temperature, small diurnal temperature variation, and a cyclic pattern of pressure variations with large amplitudes. The pressure data are plotted in Fig. 7 for a relatively quiet period in the Sol 1600's and for the 1720 to 1760 period. The 2-sol period in the pressure data for the Sol 1700's probably represents the passage of baroclinic waves with a zonal wave number of 4 to the north of the landing site. The pressure trace also demonstrates a significant diurnal solar tide associated with heating of atmospheric dust. The pressure variations were among the most prominent recorded during the mission.

During the first 2 years of observations, peak wind velocities were associated with pressure cycles having the greatest amplitudes (*10*). It is possible that when the phase of the 2-sol period wave and the solar tide combined favorably, winds could have exceeded 30 m/sec at the 1.6-m height of the meteorology boom (*12*). Thus it would appear that the changes at the landing site occurred during a relatively rare period when meteorological conditions favored strong surface winds. Partial failure of the wind velocity sensor has precluded extraction of reliable wind velocity magnitudes for this period of the mission.

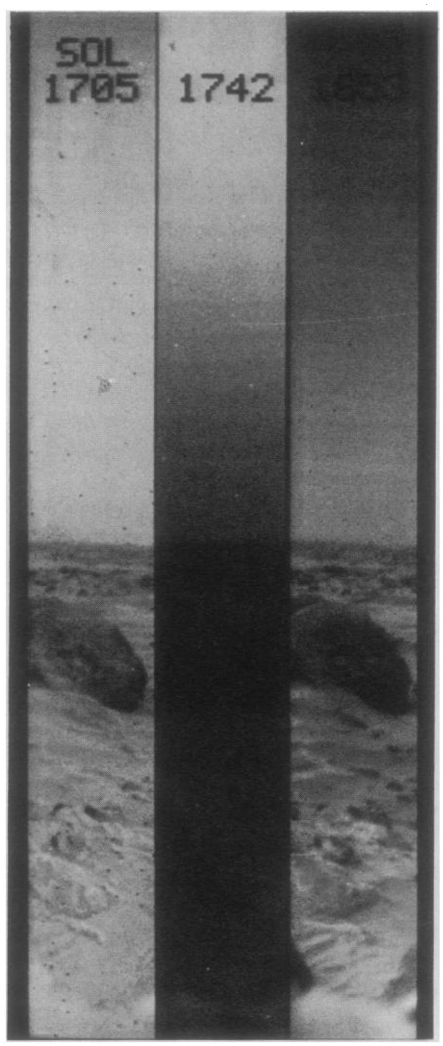

Fig. 6. Sequence of lander images acquired with the red diode of the 1-m-wide boulder Big Joe on Sols 1705, 1742, and 1853. The ratios of brightness values for the three scenes are about 1.0/0.4/0.8. The lower radiance on Sol 1742 was probably due to the abundance of aerosols (dust) in the atmosphere. (Frames J122, J127, and J142.)

Wind Velocities and Redistribution of Materials

The wind shear stress or friction velocity needed to erode loose material under martian conditions is fairly well known from both experimental and theoretical analyses (*13*). For the atmospheric conditions that prevailed during the third winter, the minimum friction velocity needed to erode loose soil with a variety of particle sizes would be approximately 1.7 m/sec. The equivalent velocity at the height of the meteorology sensors depends on the surface roughness, which is poorly defined because of the abundance and variable spacing of blocks. We estimate that winds of 25 to 30 m/sec would be needed to initiate particle motion in loose soil (*14*). When winds reach this magnitude, particles with diameters of approximately 0.2 mm could be entrained. Larger particles would be too massive to be entrained, while smaller particles would remain immobile, either because of cohesive forces or because they are within the laminar part of the boundary layer. Most likely, peak winds exceeded the minimum values of 25 to 30 m/sec during the period when the scene was extensively modified.

Upon entrainment, some particles will bounce or saltate along the surface, some will be carried into suspension, and some will travel in a surface creep mode. The maximum particle size carried in suspension depends on the relative magnitudes of the upward wind velocity component as compared to the particle settling velocity. Scaling from wind tunnel experiments (*15*), and assuming that the vertical component of wind velocity is proportional to friction velocity, we estimate that particle sizes smaller than about 0.10 mm, once entrained, would be carried aloft when winds reached the minimum friction velocity needed for entrainment. The friction velocity would have to be three times above threshold to suspend sizes corresponding to the most easily moved particles. Thus it seems probable that loose soil clods and any lithic fragments of the appropriate size (about 0.2 mm) would begin to saltate once the threshold velocity is reached. Presumably, once the most easily moved particles begin saltating, smaller particles would be stirred and carried away in suspension. The saltating particles may also have disrupted the larger (4- to 5-mm) clods and modified other parts of the scene.

It is of interest to compute a rough estimate of the rate of erosion of the piles. The rate of removal of loose material is thought to scale as the cube of the friction velocity, multiplied by a term relating the difference between the maximum and the threshold friction velocities (*16*). If, for example, the peak gust were only 10 percent above the threshold velocity, we calculate that the piles should have been removed in only a few seconds. Thus we suggest that a wind gust only slightly above threshold, and perhaps lasting only seconds, could have initiated saltation and redistributed a considerable amount of loose debris. The rest of the site should have been significantly deflated by the strong wind. The lack of such deep scouring (centimeters in depth) implies that the natural scene must be considerably more cohesive than disturbed areas. Perhaps the cohesion of the undisturbed soils restricts events of such magnitude to the outer few hundred micrometers of loose, fine-grained soil. It seems that the natural scene resists significant modification, at least for the events witnessed by the station over its 3-year observation period.

Concluding Remarks

The picture that emerges for geologic processes and weather after slightly more than 3 years of observation is one punctuated by episodic events (Fig. 8). On arrival of the spacecraft in the early northern summer, the scene was dark and contrast was high. Then two global dust storms occurred, with fallout from these storms blanketing the surface with bright red dust. During the fall and winter of the second year an additional thin layer of dust was deposited from global storms. During the winter of the third year the bright dust deposits were eroded and regions disturbed by the surface sampler were significantly modified. In the final images during the fourth fall the scene was again dark, suggesting that another storm was in progress.

From the imaging data it appears that tens to hundreds of micrometers of material are removed and deposited at the landing site over the course of a martian year. For a very brief interval over the 3 years, winds also reached sufficient velocity to erode several centimeters of disturbed materials. Apparently, much greater wind velocities are needed to reconfigure the morphology of the natural scene at the centimeter scale. As discussed, the reason may be that much of the soil is too cohesive to be eroded, even under the most extreme conditions observed during the lander mission.

In summary, the lander data imply that only rarely, under present environmental conditions, do winds reach sufficient velocities to disrupt the general scene. It is possible that once this happens, and the soil cohesion is disrupted by saltating particles, the soil deposits covering the scene may be eroded in tens of seconds. Thus the rare high-velocity event may be responsible for changing soil morphology, while winds at or only slightly above threshold may be responsible for redistributing thin surface layers. For the kinds of materials at the landing site, such events may occur so infrequently that their probability is comparable to or smaller than the probability of the atmospheric pressure increasing or decreasing significantly as the obliquity of the spin axis changes over the 10^5-year obliquity cycle (*17*). With a higher atmospheric density (about five times the present value) at high obliquity, threshold friction velocities would be closer to 1 m/sec and thus more easily attained. Erosion and deposition may then be much more common. It is possible, for instance, that the crusted surface exposed beneath the retrorocket by engine exhaust (*3*) is an erosional disconformity that is episodically reached when winds scour to centimeters in depth during periods of higher atmospheric pressure.

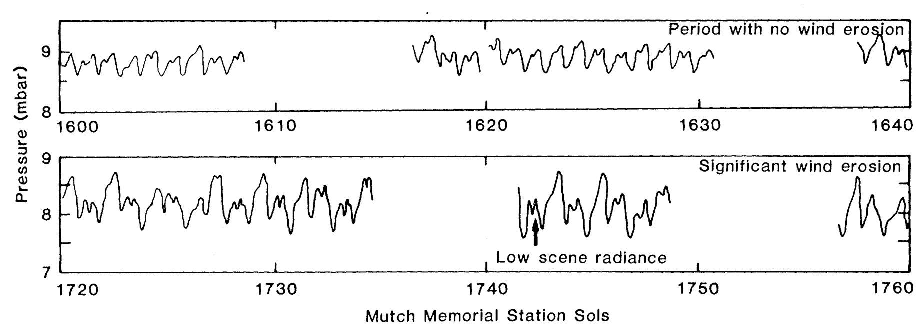

Fig. 7. Plots of atmospheric pressure for Sols 1600 to 1640 and 1720 to 1760. The earlier period corresponds to an interval when no surface changes were detected from imaging data, while the latter period corresponds to the time frame when the overall scene radiance decreased, contrast increased, the piles were eroded, and other areas were modified. The enhanced pressure oscillations for the latter period are probably due to baroclinic waves (2-sol period) and an increased diurnal amplitude due to solar tidal heating associated with suspended dust particles.

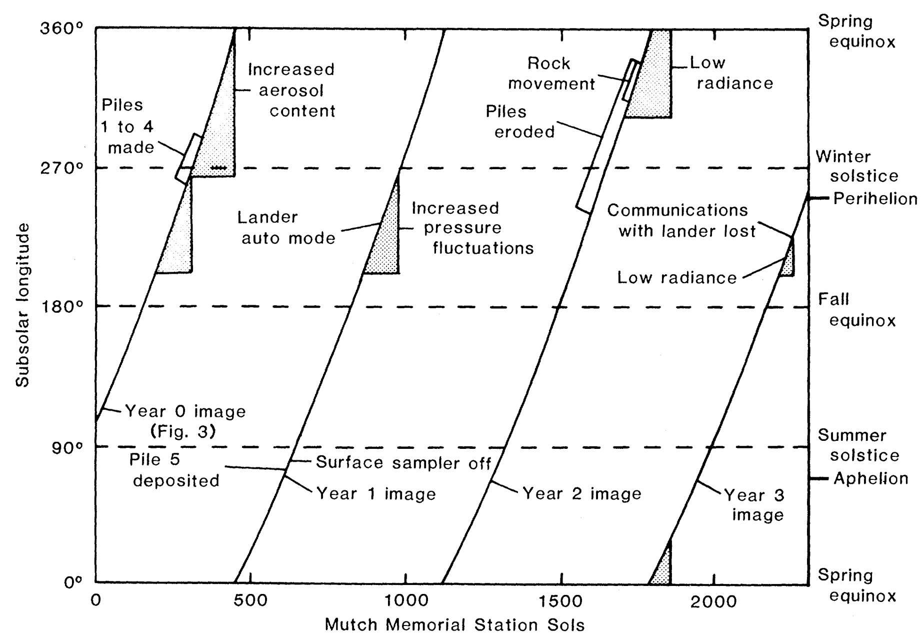

Fig. 8. Chart chronicling the timing of major scientific and engineering events associated with the mission. The ordinate is measured in degrees of subsolar longitude, with 0° representing the northern spring equinox position. The subsolar longitude is the angle between the vector connecting the sun and Mars at this position relative to the vector connecting the two bodies at any other position. The lines trending diagonally relate the number of sols after landing to the subsolar longitude. Atmospheric aerosol content was monitored from the lander by imaging the sun to obtain optical depth until Sol 921 and by monitoring pressure, temperature, and scene radiance for the remainder of the mission. Note the clustering of dust storms. Images for years 0 to 3 are displayed in Fig. 3. Significant changes in scene morphology occurred between Sols 1720 and 1757.

References and Notes

1. Thomas A. Mutch, a professor of geological sciences at Brown University and an associate administrator for space sciences at the National Atmospheric and Space Administration, was killed in a mountain climbing accident in the Himalayas in October 1980. Professor Mutch was the leader of the lander imaging team during the primary and extended missions. Contact was lost with the station after uplinking a command sequence. Repeated attempts to uplink new commands did not establish contact.
2. A sol is one martian day with a duration of 24.66 hours. When capitalized, Sol refers to a lander event time: the sol of landing is Sol 0; Sol 2238 is 2238 sols after landing. A martian year is nearly twice as long as a terrestrial year because the revolution period of Mars is 686.980 days, compared to 365.256 days for Earth.
3. Previous analyses of Viking Lander imaging data were made by E. A. Guinness, C. E. Leff, and R. E. Arvidson [*J. Geophys. Res.* **87**, 10051 (1982)]; K. L. Jones *et al.* [*Science* **204**, 700 (1979)]; H. J. Moore, R. E. Hutton, R. F. Scott, C. R. Spitzer, and R. W. Shorthill [*J. Geophys. Res.* **81**, 4497 (1977)]; H. J. Moore *et al.* [*ibid.* **84**, 8365 (1979)]; J. B. Pollack *et al.* (*ibid.*, p. 2929); and C. Sagan, D. Pieri, P. Fox, R. E. Arvidson, and E. A. Guinness [*ibid.* **82**, 4430 (1977)].
4. The Viking Lander meteorology experiment was described by S. L. Hess, R. M. Henry, C. B. Leovy, J. Ryan, and J. Tillman [*J. Geophys. Res.* **82**, 4559 (1977)].
5. The lander camera system was described by W. R. Patterson, F. O. Huck, S. D. Wall, and M. R. Wolf (*ibid.*, p. 4391). There are two identical cameras on each lander, spaced 0.8 m apart and standing 1.3 m above the surface. The cameras work by acquiring one vertical scan line with a nodding mirror. The light is focused onto a photodiode array, and the image is constructed by rotating the assembly about a vertical axis between each scan line. Six diodes were used for multispectral imaging in the 0.5- to 1.0-μm region, with an angular resolving power of 0.12°, while another suite of diodes was used for broadband (peak in red) imaging at 0.04° angular resolving power. Another diode was used for broadband, low-resolution (0.12°) imaging. In addition, one diode was used to obtain atmospheric optical depth by imaging of the sun. The sensor output voltages were coded to a range of 64 brightness units and the data were either telemetered directly back to Earth or stored for later relays.
6. Images acquired in support of sampler activities were described by S. Liebes, Jr., and A. A. Schwartz (*ibid.*, p. 4421).
7. J. A. Ryan, R. D. Sharman, R. D. Lucich, *Geophys. Res. Lett.* **8**, 899 (1981); P. B. James and N. Evans, *ibid.*, p. 903.
8. To detect changes in brightness and contrast during the observations the radiometric responses of the lander cameras must not drift or the drift must be checked. Drift in camera preamplifier voltages for the blue, green, red, and three infrared diodes was monitored on a regular basis for the first 921 sols on Mars, until the station was commanded to an automatic state. On command, the camera lens was covered by a black flag and the diode responses were measured. Next, each diode response to a lamp was measured. Except for the infrared channels, the change in preamplifier voltage, corrected for diode temperature, was negligible for this period. Extrapolation to the end of the mission suggests that the drift would be less than one brightness unit.
9. The brightness in shadowed areas varied between the frames by only 1 to 2 units, while the cameras recorded a range of 64 units for each frame.
10. C. Leovy, *J. Atmos. Sci.* **38**, 39 (1981); J. A. Ryan and R. D. Sharman, *J. Geophys. Res.* **86**, 3247 (1981).
11. Soil in this case refers to fine-grained debris, with no connotations as to organic content. Particle sizes for the soils exposed at the station are thought to be in the clay to silt size range. Clods composed of these fine-grained soils up to centimeters in width can be seen in the images, and their cohesion varies. Thus, a spectrum of particle sizes exists. See H. J. Moore *et al.* [*J. Geophys. Res.* **84**, 8365 (1979); *ibid.* **87**, 1043 (1982)] for a summary of soil properties.
12. C. Leovy, personal communication.
13. The friction velocity is the square root of the ratio of wind shear stress to atmospheric density. The wind velocity at some height above the surface is related to the friction velocity and the distribution of surface roughness elements. Theoretical and experimental work [R. Greeley, R. Leach, B. White, J. Iversen, J. Pollack, *Geophys. Res. Lett.* **7**, 121 (1980); J. Iversen, R. Greeley, J. Pollack, *J. Atmos. Sci.* **33**, 2425 (1976)] was used to compute the threshold friction velocity quoted in text for atmospheric conditions in the late winter.
14. J. L. Sutton, C. B. Leovy, and J. Tillman [*J. Atmos. Sci.* **35**, 2346 (1978)] suggested that surface roughness values from 0.1 to 1.0 cm might be appropriate. These estimates and the Von Karman relation for a fully turbulent boundary layer indicate that winds with velocities of 25 to 30 m/sec are needed to erode loose soil. An equally plausible interpretation is that the 4- to 5-mm particles were moved directly by strong winds between Sols 1720 and 1757. In this case, threshold friction velocities of 3 to 5 m/sec and wind velocities of 40 to 90 m/sec would be needed.
15. J. B. Pollack, R. H. Aberle, R. Greeley, J. Iversen, *Icarus* **29**, 395 (1976).
16. B. White, *J. Geophys. Res.* **84**, 4643 (1979).
17. O. B. Toon, J. B. Pollack, W. Ward, J. A. Burns, K. Bilski, *Icarus* **44**, 552 (1980).

18. We are indebted to the small but highly motivated crew at Jet Propulsion Laboratory that operated the Mutch Memorial Station and provided data. We thank G. N. Gianopulos, A. Britting, Jr., J. P. Brinkle, Esche, D. Pieri, and K. L. Jones. Thanks are also extended to S. LaVoie, whose perseverance in the face of limited funds provided us with data. Support was provided by the Planetary Geology and the Mars Data Analysis Programs, NASA Headquarters. Finally, deep thanks are extended to J. Boyce and H. Brinton for continued interest in the findings of the Mutch Memorial Station.

Relaxed Cellular Controls and Organelle Heredity

C. William Birky, Jr.

DNA molecules carrying small but vitally important sets of genes have been demonstrated in the chloroplasts of plants and algae, and in the mitochondria of protists, fungi, plants, and animals (*1*–*3*). The inheritance of these mitochondrial and chloroplast genes has been studied in all of the eukaryotic kingdoms, so that it is now possible to identify the truly general features of organelle gene transmission, segregation, and recombination (*4*). Of special interest and importance are phenomena that are characteristic of mitochondrial and chloroplast genes and distinguish their behavior from that of genes in the nucleus. They are often transmitted from only one parent, and alleles segregate during mitotic cell divisions. Much effort has been devoted to analyzing the cellular and molecular mechanisms which underlie and explain these phenomena.

There is still no general agreement about these mechanisms or about their evolutionary significance. Several different hypotheses have been proposed, none of which is sufficiently general to encompass the phenomena seen in different organisms. However, recent genetic studies have suggested an underlying theme that relates the inheritance of organelle genes to a lack of stringent cellular control over the behavior of organelles and organelle DNA.

C. William Birky, Jr., is a professor in the Department of Genetics and the Program in Molecular, Cellular, and Developmental Biology at Ohio State University, Columbus 43210.

Phenomena to Be Explained

The most important and singular features of organelle heredity are uniparental inheritance and vegetative segregation (*4*). These phenomena are illustrated by crosses of green and mutant white chloroplasts in the geranium (*3*) (Fig. 1A). When a plant with green plastids in its germ-line cells is crossed to a plant with mutant white germ-line plastids, three kinds of zygotes are produced, in varying proportions: (i) uniparental (maternal) zygotes, which develop into plants with only green plastids; (ii) uniparental (paternal) zygotes, which give rise to plants with only white plastids (these plants die as seedlings); and (iii) biparental zygotes, which produce variegated plants having sectors of green and white cells. The first two classes show uniparental inheritance in that they develop into plants that contain chloroplast genes from only one parent.

The young plants arising from biparental zygotes have mixed cells that contain both green and white plastids; but each cell in the mature variegated plant is homoplasmic (homozygous for cytoplasmic genes), containing only green or only white plastids. These cells are the result of vegetative segregation—that is, the segregation of wild-type and mutant al-